

Conversion of benzoic acid during TiO₂-mediated photocatalytic degradation in water

Theodora Velegraki, Dionissios Mantzavinos*

Technical University of Crete, Department of Environmental Engineering,
Polytechniopolis, GR-73100 Chania, Greece

Received 6 June 2007; received in revised form 13 August 2007; accepted 21 August 2007

Abstract

The photocatalytic degradation of benzoic acid in water over Degussa P-25 TiO₂ suspensions was studied. UVA irradiation at 365 nm was supplied by a medium pressure mercury lamp providing 25 mW cm⁻² light intensity. Experiments were conducted at benzoic acid initial concentrations between 25 and 150 mg L⁻¹, catalyst loadings between 0.2 and 1 g L⁻¹ and initial solution pH values between 2 and 10.6. Conversion increased with increasing catalyst loading up to about 0.6 g L⁻¹ and it was favored at alkaline or neutral conditions but impeded at extremely acidic conditions. Increasing initial substrate concentration led to decreased benzoic acid conversion, which was found to follow a Langmuir–Hinshelwood kinetic expression. High performance liquid chromatography (HPLC) was employed to follow benzoic acid concentration profiles as well as to identify reaction by-products, while chemical oxygen demand (COD) and total organic carbon (TOC) analyses were carried out to assess the extent of mineralization. Benzoic acid hydroxylation by-products, namely 2-, 3- and 4-hydroxybenzoic acids as well as phenol were identified as reaction intermediates, although these contributed only a small fraction of the residual organic content. Although benzoic acid at 50 mg L⁻¹ was not ecotoxic to marine photobacteria *Vibrio fischeri*, its photodegraded solution exhibited substantial toxicity, which, however, proved not to be due to the identified intermediates.

© 2007 Elsevier B.V. All rights reserved.

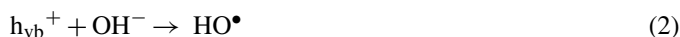
Keywords: Benzoic acid; Intermediates; Photocatalysis; Titanium dioxide; Toxicity

1. Introduction

Heterogeneous photocatalysis is an advanced oxidation process where semiconductors, acting as catalysts, are exposed to UV irradiation. Photocatalytic degradation occurs through a multistep process that involves the formation of reactive species on the surface of the photocatalyst and the subsequent generation of hydroxyl radicals that result in the mineralization of most organic compounds. The most extensively used photocatalyst is titanium dioxide due to its optical and electronic properties, low cost, abundance, chemical stability and non-toxic nature. The TiO₂-mediated photocatalysis has been successfully employed to oxidize many organic pollutants present in aqueous systems that cannot be treated by conventional techniques due to their chemical stability and/or low biodegradability [1,2].

In brief, the mechanism of heterogeneous photocatalytic degradation can be described as follows: illumination of an aque-

ous TiO₂ suspension with irradiation with energy greater than the band gap energy of the semiconductor (i.e. 3.2 eV in the case of anatase TiO₂) generates valence band holes (h_{vb}⁺) and conduction band electrons (e_{cb}⁻). Due to this wide gap energy, TiO₂ can be activated by UVA irradiation below 385 nm. Holes and electrons may either undesirably recombine liberating heat or make their separate ways to the surface of TiO₂, where they can react with species adsorbed on the catalyst surface. Valence band holes can react with water and the hydroxide ion (e.g. under alkaline conditions) to generate hydroxyl radicals HO[•], while electrons can react with adsorbed molecular oxygen reducing it to superoxide radical anion which, in turn, reacts with protons to form peroxide radicals:



* Corresponding author. Tel.: +30 2821037797; fax: +30 2821037852.
E-mail address: mantzavi@mred.tuc.gr (D. Mantzavinos).

Organic compounds can then undergo both oxidative degradation through their reactions with valence band holes, hydroxyl and peroxide radicals and reductive cleavage through their reactions with electrons yielding various by-products and eventually mineral end-products.

The target compound employed in this study is benzoic acid as it constitutes the parent molecule of many phenolic compounds such as vanillic, gallic, veratric, syringic, protocatechuic and hydroxybenzoic acids that are commonly found in agro-industrial effluents which, like olive mill wastewaters, are usually characterized by low biodegradability and high ecotoxicity [3]. In the form of its ester, benzoic acid is widely used in the food and pharmaceutical industry as an antimicrobial preservative frequently included in liquid forms and personal care products.

Benzoic acid photocatalytic degradation has merely been studied in recent years. Vione et al. [4] demonstrated the superiority of a commercially available white pigment containing TiO₂ over Degussa P-25 to degrade model aqueous solutions of (primarily) phenol and benzoic acid, while Mehrotra et al. [5] elucidated the intrinsic kinetic parameters of photocatalytic degradation in a monolithic-type reactor with immobilized Degussa P-25. Di Paola et al. [6] studied the effect of TiO₂ doping with several metals on its activity to degrade several organics including benzoic acid amongst others. However, relatively little is known about the effect of operating conditions on conversion and predominantly about the elucidation of reaction intermediates as well as the effect of photocatalytic treatment on subsequent toxicity.

The present work deals with the investigation of several parameters that affect the efficiency of the photocatalytic degradation of benzoic acid such as the loading of the catalyst, the initial concentration of the model compound and the initial pH of the aqueous solution. Reaction intermediates are identified and partly quantified, while the ecotoxicity of the solution during and after treatment is evaluated. Moreover, the contribution of the identified intermediate compounds to toxicity is explored.

2. Experimental and analytical

2.1. Materials

Benzoic acid (>99.5%) has been obtained by Fluka and used without further purification. HPLC-grade acetonitrile and *ortho*-phosphoric acid 85% were supplied by Riedel de Haën. Potassium dihydrogen phosphate (>99.5%) was supplied by Merck. All reaction mixtures and HPLC mobile phase solutions were prepared in double distilled water (EASYpureRF, Barnstead/Thermolyne, USA). TiO₂ Degussa P-25 supplied by Degussa AG (anatase/rutile: 65/35, non-porous, mean size 30 nm, surface area 56 m² g⁻¹) was employed as photocatalyst in this study.

2.2. Irradiation procedure

Experiments were carried out in a cylindrical reaction vessel, batch type, coupled with a double-walled immersion well

with inlet and outlet tubes for cooling, both made of borosilicate glass and purchased from Ace Glass, USA. Prior to each experiment, 350 mL aqueous solution of known concentration of the model compound was introduced into the reaction vessel, along with known amount of titanium dioxide powder. The temperature of the reaction mixture was maintained constant at 28 ± 2 °C throughout the photocatalytic experiments. The solution was equilibrated by magnetic stirring for 30 min in the dark to ensure complete equilibration of adsorption/desorption of organic compounds on the catalyst surface before exposing the reactor assembly to the concentrated UV light [1]. At the end of this period, a sample of 5 mL was withdrawn, filtered and analyzed to determine the equilibrium concentration which was used to compute benzoic acid conversion. In most cases, experiments were performed at ambient pH (3.8) which was not controlled during the reaction. In those cases where runs were carried out at basic, neutral or extremely acidic pH, the initial pH was adjusted by adding the appropriate amount of NaOH or HCl. Air was sparged in the liquid at all times to keep all the TiO₂ in suspension and to assure that oxygen pre-saturation of the solution had been reached prior to the activation of a medium pressure mercury vapor lamp at 125 W (Kolorlux) which emits predominantly at 365 nm. Emission below 300 nm is impeded due to the construction material of the reactor. Samples were withdrawn at fixed intervals through PTFE tubing (6 mm) and with the use of a centrifugal pump and were immediately filtered (0.45 μm, Nylaflo, PALL) to remove TiO₂ particles. The entire set-up was placed inside a fume put chamber for security reasons and in order to eliminate any interference of additional light sources. The reactor was thoroughly covered with aluminium foil in order to exploit the scattered UV radiation. The incident radiation in solution in the UV region was 28 mW cm⁻² as measured with an ACCU-CAL-50 radiometer (DYMAX Corporation).

2.3. Analytical determinations

Liquid samples were analyzed with respect to their composition by means of an HPLC system (Shimadzu) equipped with diode array (SPD-M10A_{Vp}) and fluorescence (RF-10A_{XL}) detectors, two solvent LC-10AD_{Vp} delivery pumps and an autosampler (SIL-10AD_{Vp}). Benzoic acid and its reaction intermediates were separated on a reverse-phase C-18 column (Prevail Organic Acid, 250 mm × 4.6 mm) using a mixture of acetonitrile (MeCN, 30%) and phosphate buffer solution 25 mM pH 2.6 (KH₂PO₄, 70%) as the mobile phase. Aliquots of 20 μL were injected and eluted isocratically at a flow rate of 1 mL min⁻¹ and ambient temperature. Benzoic acid was detected at 230 nm, whereas the intermediates were detected at 210 nm. The identity of an intermediate compound was established by comparing its retention time and UV spectrum with that of a standard compound. External standards were prepared with known concentrations of the supposed compounds either separately or in mixture. The linearity between absorbance and concentration was tested using external standards at various concentrations and the response was found to be linear over the whole range of concentrations under consideration. Blank sam-

ples were run between two consecutive HPLC runs to ensure that no residuals from the previous run were carried over to the next run. The inter-day repeatability of the method was found to be excellent with a relative standard deviation of 0.9%.

A TOC 5000A Shimadzu Analyzer was used to perform total organic carbon determination and to evaluate the extent of mineralization that had occurred. Its operation is based on the combustion/non-dispersive infrared gas analysis. Total carbon (TC) was first measured and then the inorganic carbon (IC) was measured. The TOC was determined by subtracting IC from TC. pH was determined with a Crison GLP 21 pH meter. COD was determined colorimetrically according to the EPA approved reactor digestion method [7] in order to monitor the COD reduction of the solution during degradation. The appropriate amount of sample was introduced into commercially available digestion solution in the range 0–150 mg L⁻¹ containing potassium dichromate, sulfuric acid and mercuric sulfate (Hach Europe, Belgium) and the mixture was then incubated for 120 min at 150 °C in a COD reactor (Model 45600-Hach Company, USA). COD concentration was measured colorimetrically at 620 nm using a DR/2010 spectrophotometer (Hach Company, USA).

2.4. Toxicity evaluation

The luminescent marine bacteria *Vibrio fischeri* were used to assess the acute ecotoxicity of benzoic acid samples collected at fixed intervals during the photodegradation process. The inhibition of *V. fischeri* was measured by the Microtox test system (Microtox 500 Analyzer (SDI, USA)) at exposure times of 15 and 30 min. Luminescent bacteria emit light as a by-product of their cellular respiration and metabolic processes. During contact with the target compounds, the reduction in the light emission indicates a decrease in the respiration rate, due to the presence of toxic substances. The pH of the samples was adjusted to 7 ± 1 prior to toxicity tests with the addition of 0.1N HCl or 0.1N NaOH solutions, so that pH-related light inhibition was avoided. Furthermore, NaCl was added to the sample at 2% (w/v) concentration to exclude light inhibition due to osmotic phenomena.

3. Results and discussion

Before the start of the photocatalytic reactions, preliminary experiments were conducted to investigate whether any direct photolysis would take place. Benzoic acid was found to be photostable in the absence of catalyst, which is in good agreement with previous reports [5,8]. Moreover, mixing benzoic acid with the catalyst in the absence of light led to a slight concentration decrease in the order of 10% presumably due to the adsorption of the organic compound onto the catalyst surface.

3.1. Effect of catalyst concentration

The influence of catalyst loading on the abatement of benzoic acid has been investigated using different concentrations of TiO₂ varying from 0.2 to 1 g L⁻¹ and the results are presented in Fig. 1. In terms of complete substrate conversion, decom-

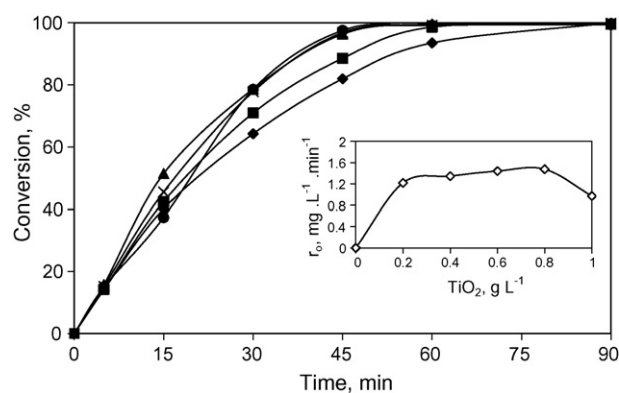


Fig. 1. Benzoic acid conversion during photocatalytic treatment at various concentrations of Degussa P-25: (♦) 0.2 g L⁻¹; (■) 0.4 g L⁻¹; (▲) 0.6 g L⁻¹; (×) 0.8 g L⁻¹; (●) 1 g L⁻¹. Inset: dependence of the initial reaction rate r_0 on the concentration of the catalyst. Initial solution pH: 3.8; substrate initial concentration: 50 mg L⁻¹.

position increases with increasing catalyst concentration up to a value of 0.6 g L⁻¹ where complete conversion occurs within 45 min of reaction. Degussa P-25 is a highly photoreactive catalyst whose activity is generally attributed to a slow electron/hole recombination rate [9–11]. At catalyst loadings above 0.6 g L⁻¹ no significant improvement is obtained. As the amount of catalyst particles inside the solution increases, more photons are adsorbed onto the catalyst surface, thus accelerating the degradation process. The optimum concentration of the catalyst depends strongly on the catalyst type, photoreactor geometry and the operating conditions employed [12,13]. The leveling off at catalyst concentrations over 0.6 g L⁻¹ (e.g. at 30 and 45 min of reaction) implies that there are already enough catalyst particles (i) for the unconverted molecules to adsorb on and undergo degradation and (ii) to induce the formation of sufficient concentrations of hydroxyl radicals and other reactive moieties that could then attack the substrate in the liquid bulk. In this view, further addition of catalyst particles does not improve degradation rates. Moreover, the excess of TiO₂ particles could hinder degradation by increasing the opacity of the suspension, thus increasing light reflectance [14]. This seems to occur during the early stages of the reaction; as seen in the inset of Fig. 1, the initial degradation rate (r_0 calculated over the first 15 min) does not practically change as the catalyst concentration increases from 0.6 to 0.8 g L⁻¹ but slightly decreases when concentration increases to 1 g L⁻¹. Therefore, all subsequent experiments were conducted at a catalyst concentration of 0.6 g L⁻¹.

3.2. Effect of initial pH

Fig. 2 shows the influence of the initial pH of the irradiated solution on the conversion of benzoic acid. The initial pH values varied from strongly acidic conditions (e.g. pH 2) through natural and neutral conditions of pH 3.8 and 7.5 respectively up to alkaline conditions (e.g. pH 10.6). Titanium dioxide exhibits an amphoteric character, so that either a positive or a negative charge can be developed on its surface [1]. The point of zero charge for Degussa P-25 is at pH ≈ 6 above and below which the TiO₂ surface becomes negatively and positively charged,

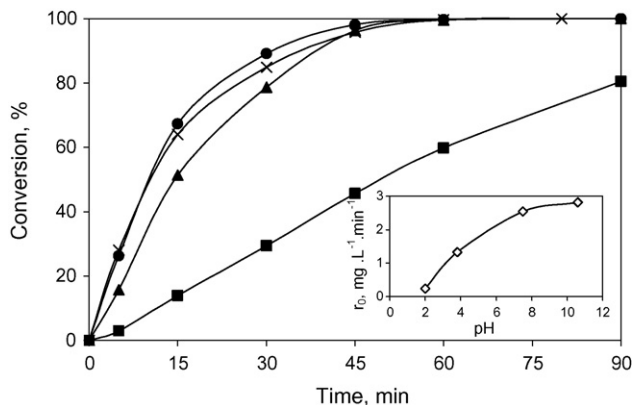


Fig. 2. Benzoic acid conversion during photocatalytic treatment at various initial pH values: (●) pH 7.5; (×) pH 10.6; (▲) pH 3.8 natural; (■) pH 2. Inset: dependence of the initial reaction rate r_0 on the initial pH of the solution. Substrate initial concentration: 50 mg L^{-1} ; Degussa P-25: 0.6 g L^{-1} .

respectively. Blank runs were performed to assess the extent of dark adsorption at various pH values and this was found to be about 15% at pH 3.8 (natural) and 2, while adsorption at neutral and alkaline conditions was found to be insignificant. Benzoic acid, a weak acid whose pK_a is 4.2, exists partly in its anionic state and, therefore, an electrostatic attraction is expected to develop between the pollutant and the positively charged catalyst particles at $\text{pH} < 6$. The extent of substrate adsorption onto the catalyst would then be favored at $4.2 < \text{pH} < 6$ (i.e. most of the substrate is in the form of benzoate) and expectedly decrease at $\text{pH} < 4.2$ which is consistent with the relatively low levels of adsorption recorded at strongly acidic conditions. On the other hand, no adsorption was recorded at $\text{pH} > 6$ as both catalyst and the substrate are negatively charged. Although one might have expected that photocatalytic degradation would have been favored at acidic conditions, conversion decreases with decreasing initial solution pH and this is more pronounced during the early stages of the reaction as demonstrated by the dependence of initial reaction rates on solution pH (inset of Fig. 2).

Since benzoic acid adsorption onto catalyst is not favored at neutral or alkaline conditions, its degradation appears to proceed via reactions with hydroxyl radicals in the liquid bulk. The beneficial role of high pH values on degradation may then be ascribed to the increased production of hydroxide anions, which in turn facilitate the photogeneration of hydroxyl radicals according to reaction (2) [15,16]. It should be noticed here that as the reaction proceeds, solution pH drops presumably due to the formation of acidic by-products (it should be borne in mind that solutions were adjusted but not buffered to their starting pH values) and this drop was more pronounced for the experiments carried out at alkaline or neutral conditions. Therefore, it is not surprising why the extent of benzoic acid conversion after 45–60 min is nearly 100% for initial pH values of 3.8 and 10.6 although the respective initial rates have a threefold difference.

A possible explanation for the reduced conversion rates observed at highly acidic conditions may involve the decrease of the available active centers on the catalyst surface, which in turn causes a reduction of the adsorbed photons. Moreover, the electrostatic attraction developed between the positively charged

catalyst particles and benzoate could have caused the formation of a multilayer of organic molecules around the catalyst particles without permitting many of these molecules to come to direct contact with the catalyst, thus resulting in slower degradation rates [1].

3.3. Effect of initial substrate concentration

The effect of initial benzoic acid concentration was studied employing four different values, namely 25, 50, 100 and 150 mg L^{-1} at a constant catalyst loading of 0.6 g L^{-1} and natural pH 3.8. Fig. 3 shows temporal changes of equilibrium concentration (C_{eq}) and, as seen, conversion decreases with increasing initial substrate concentration; for instance, complete conversion is achieved after 30, 45 and 90 min of reaction at 25, 50 and 100 mg L^{-1} , respectively. This could be related to the formation of several layers of adsorbed organic molecules onto the particles surface, which becomes more pronounced as concentration increases. The adsorbed molecules cannot easily come to direct contact with the photogenerated holes or hydroxyl radicals, thus resulting in slower conversion. Furthermore, as the initial concentration increases the path length of photons entering the solution decreases, which results in lower photon adsorption on catalyst particles and as a consequence in lower photocatalytic reaction rates [17]. However, it should be pointed out that, unlike conversion, process efficiency in terms of mass of benzoic acid degraded increases at higher initial concentrations. For instance, the amount of substrate removed after 90 min of reaction is 20, 42, 82 and 100 mg L^{-1} at 25, 50, 100 and 150 mg L^{-1} initial concentration, respectively.

Photocatalytic degradation usually follows a Langmuir–Hinshelwood kinetic model described by the equation:

$$\frac{1}{r_0} = \frac{1}{k_r K C_{eq}} + \frac{1}{k_r} \quad (5)$$

where K is the equilibrium constant for adsorption of the organic substrate onto TiO_2 surface and k_r is the rate of reaction. The reciprocal of the initial rate is plotted against the reciprocal of

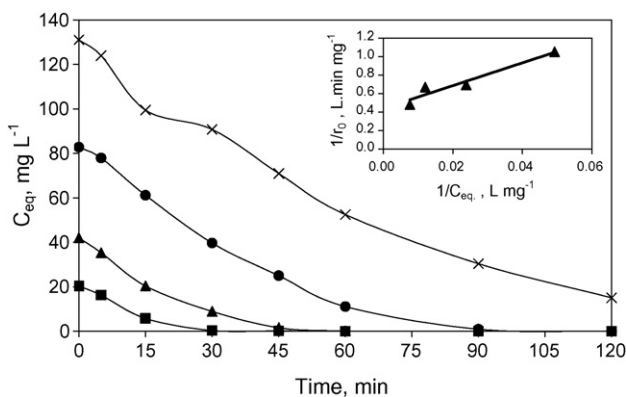


Fig. 3. Benzoic acid temporal profiles during photocatalytic treatment at various initial concentrations: (■) 25 mg L^{-1} ; (▲) 50 mg L^{-1} ; (●) 100 mg L^{-1} ; (×) 150 mg L^{-1} . Inset: plot of Eq. (5). Initial solution pH: 3.8; Degussa P-25: 0.6 g L^{-1} .

the equilibrium concentration in the inset of Fig. 3 and the K and k_r values computed from the slope and intercept of the resulting straight line are 0.028 L mg^{-1} and $2.23 \text{ mg (L min)}^{-1}$, respectively.

3.4. Determination of reaction intermediates

Four major intermediates accompanying the photocatalytic decomposition of benzoic acid were identified by means HPLC/DAD analysis, namely 2-, 3- and 4-hydroxybenzoic acids (HBAs) and phenol. Fig. 4 shows temporal profiles of all four identified intermediates in terms of concentration and/or chromatographic peak areas. For the three monohydroxybenzoic acids, profiles were taken from a photocatalytic experiment at 50 mg L^{-1} benzoic acid whose concentration–time profile (divided by a factor of 10 for clarity) is also shown in Fig. 4. For phenol, its profile was taken from a run at 150 mg L^{-1} benzoic acid concentration as it could not be detected accurately at lower initial substrate concentrations. All three HBAs reach their maximum concentration after 15 min of reaction at which point the parent compound has been converted by about 70% and then decompose to form other by-products. Of these, 4-HBA is the dominant, in terms of concentration compound, while 3-HBA and 2-HBA are formed at lower concentrations. Quantification was possible for 3-HBA and 4-HBA, whereas 2-HBA and phenol were formed at concentrations below the method's quantification limit of 1 mg L^{-1} and, therefore, quantification was not plausible. After 15 min of reaction, 4-HBA and 3-HBA have been detected at concentrations of 1.6 and 0.9 mg L^{-1} , respectively, while at the same time the remaining concentration of benzoic acid is about 14 mg L^{-1} . The formation of HBAs could be explained through hydroxylation of benzoic acid at the *ortho*-, *para*- and *meta*-position and this is in good agreement with results reported by Chan et al. [18], Deng et al. [19] and Matthews [20,21].

In addition to the aforementioned detected compounds, another chromatographic peak, whose profile is also shown in Fig. 4, appears to correspond to a major intermediate (in terms

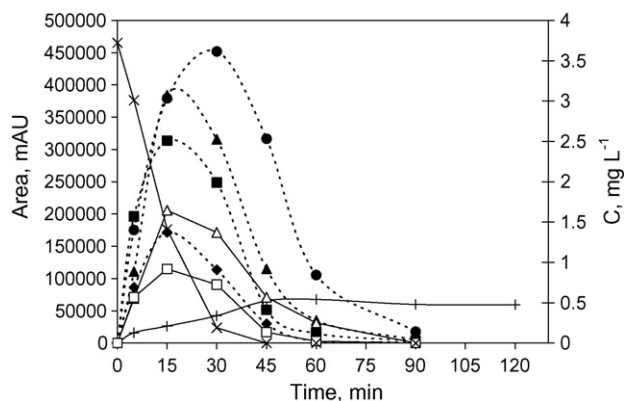


Fig. 4. Evolution of intermediate compounds during photocatalytic conversion of benzoic acid: (●) unidentified intermediate; (▲ and △) 4-HBA; (■ and □) 3-HBA; (◆) 2-HBA; (×) benzoic acid divided by a factor of 10; (+) phenol. Initial solution pH: 3.8; Degussa P-25: 0.6 g L^{-1} . Closed symbols refer to left axis, while open symbols refer to right axis.

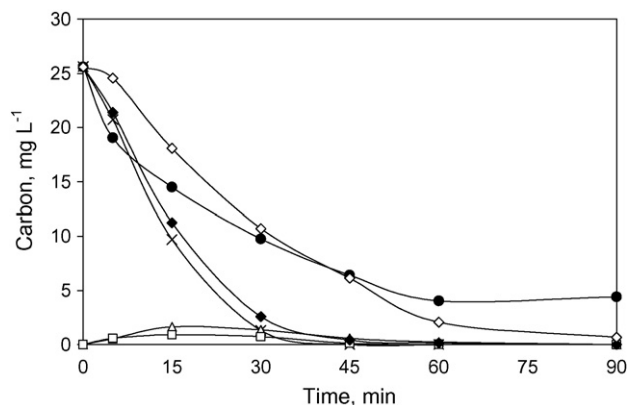


Fig. 5. Carbon concentration profiles for (×) benzoic acid; (△) 4-HBA; (□) 3-HBA; (●) TOC; (◆) TCOC; (◇) sum of TCOC and unidentified compound. Substrate initial concentration: 50 mg L^{-1} ; initial solution pH: 3.8; Degussa P-25: 0.6 g L^{-1} .

of chromatographic peak area) of benzoic acid degradation. Although determination was not possible with the analytical techniques employed in this study, it is suspected that this peak may correspond to a short-chain organic acid since (i) it remains at relatively high concentrations even after 30–45 min of reaction where all of the original benzoic acid and most of its aromatic by-products have already been converted, thus implying cleavage of the aromatic ring and (ii) it does not absorb appreciably above 210 nm. To check for this hypothesis, solutions of several carboxylic acids, namely oxalic, formic, acetic, lactic, maleic and succinic were prepared and analyzed by HPLC/DAD but unfortunately none of them matched the retention time of the unknown compound.

Fig. 5 shows temporal TOC profile during the photocatalytic degradation of 50 mg L^{-1} benzoic acid solution where 85% mineralization can be achieved after 60 min of reaction. In addition, Fig. 5 shows carbon concentration profiles for the three identified and quantified compounds (i.e. residual benzoic acid, 3-HBA and 4-HBA) as well as the total calculated organic carbon (TCOC) which is defined as the sum of the organic carbon contributions calculated from all the detected and identified compounds. The discrepancy between TOC and TCOC corresponds to the intermediate compounds that could not be detected and/or quantified with the analytical protocols employed in this study. During the early stages of the reaction, this discrepancy is relatively low (i.e. about 20% for the sample taken after 15 min of reaction), which implies that the organic carbon contained in the unreacted benzoic acid and its detected intermediates accounts for most of the sample's organic content; after prolonged irradiation though (i.e. 30–45 min), the discrepancy rises to 75–90% and this is believed to be due to the fact that short carboxylic acids and possibly other end-products could not be identified.

An attempt was made to evaluate the contribution of the unknown intermediate compound to the carbon balance. In view of this and given that the various acids tested, namely oxalic, acetic, lactic, maleic and succinic have a similar chromatographic response factor (i.e. peak area to concentration ratio) of $1.2 \pm 0.2 \times 10^{-5}$ it was assumed that the unknown compound

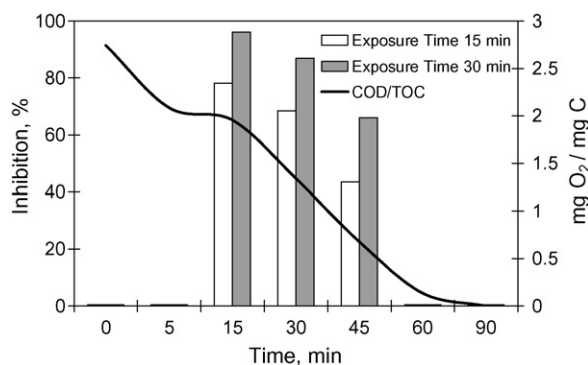


Fig. 6. Acute ecotoxicity (left axis) and COD/TOC ratio (right axis) evolution as a function of irradiation time. Substrate initial concentration: 50 mg L^{-1} ; initial solution pH: 3.8; Degussa P-25: 0.6 g L^{-1} .

will also have a similar response factor and this was taken equal to 1.2×10^{-5} . Moreover, its carbon content was taken equal to the mean value of the carbon contents of the various acids (lying between 19 and 43% for oxalic and lactic acids, respectively). Based on these assumptions, the carbon profile of the unknown compound could be extracted and added to the TCOC profile. Comparison between TOC and the sum of TCOC and the carbon contribution from the unknown compound (Fig. 5) shows that a good estimate of the carbon balance was achieved.

3.5. Acute ecotoxicity evolution

The acute ecotoxicity to *V. fischeri* of 50 mg L^{-1} benzoic acid solutions prior to and after photocatalytic treatment was monitored as a function of irradiation time and the results are shown in Fig. 6. Although the original solution is non-toxic to the specific test organism at 50 mg L^{-1} substrate concentration, toxicity appears to increase considerably upon irradiation and the 30 min-exposure time inhibition takes values of 96 and 87% after 15 and 30 min of reaction, respectively (the 15 min-exposure time inhibition is expectedly lower but still high); this timescale coincides with the major intermediates reaching their maximum concentration in the reaction mixture (see Fig. 4). As reaction proceeds further, toxicity decreases and the solution becomes non-toxic after 60 min presumably due to the decomposition of reaction by-products which are eventually mineralized to carbon dioxide and water. This is also demonstrated in Fig. 6, which shows temporal changes of COD/TOC ratio; from a starting value of 2.7, the ratio decreases to 0.68 and 0.14 after 45 and 60 min of reaction.

To evaluate whether increased ecotoxicity was due to the major intermediates accompanying benzoic acid degradation, samples containing each of the three HBAs at concentrations similar to those present in the reaction mixture after 30 min of irradiation were prepared and tested showing no ecotoxicity. Moreover, a sample containing phenol at a concentration of 1 mg L^{-1} (i.e. this value corresponds to the HPLC quantification limit for phenol) and the three detected HBAs together with benzoic acid was also prepared and tested to exclude the possibility of increased toxicity being due to synergistic or antagonistic effects among the various molecules [22]; likewise, no ecotox-

icity was recorded. Therefore, it is hypothesized that sample ecotoxicity may be due to the unknown intermediate detected in the reaction mixture and/or the presence of other products that could not be detected.

4. Conclusions

The conclusions drawn from this study are summarized as follows:

- (1) Benzoic acid photocatalytic degradation occurs relatively easily and, in general, complete conversion can be achieved in less than about 60 min of UVA irradiation in the presence of titanium dioxide. Conversion is a strong function of the operating conditions employed, namely, loading of the photocatalyst, solution pH and initial substrate concentration.
- (2) Degradation is accompanied by the formation of several reaction by-products; of these, three monohydroxybenzoic acids and phenol were successfully identified and/or quantified, while another major intermediate that could not be determined is believed to be a ring-cleavage compound. Deep oxidation results in nearly complete mineralization of the organic carbon to carbon dioxide and water.
- (3) Acute ecotoxicity to marine bacteria *V. fischeri* increases sharply during the early stages of the reaction although the original substrate is hardly ecotoxic to the specific test organism at the concentration range in question. This toxicity cannot be attributed to the major reaction by-products that have been identified and, therefore, it is likely to be associated with the residual, unidentified organic matter. Deep oxidation progressively removes ecotoxicity.

Acknowledgments

This work is part of the 03ED375 research project, implemented within the framework of the "Reinforcement Programme of Human Research Manpower" (PENED) and co-financed by National and Community Funds (75% from E.U.-European Social Fund and 25% from the Greek Ministry of Development-General Secretariat of Research and Technology).

References

- [1] E. Bizani, K. Fytianos, I. Poullos, V. Tsiroidis, Photocatalytic decolorization and degradation of dye solutions and wastewaters in the presence of titanium dioxide, *J. Hazard. Mater.* 136 (2006) 85–94.
- [2] M. Hincapié, M.I. Maldonado, I. Oller, W. Gernjak, J.A. Sánchez-Pérez, M.M. Ballesteros, S. Malato, Solar photocatalytic degradation and detoxification of EU priority substances, *Catal. Today* 101 (2005) 203–210.
- [3] W. Gernjak, M.I. Maldonado, S. Malato, J. Cáceres, T. Krutzler, A. Glacer, R. Bauer, Pilot-plant treatment of olive mill wastewater (OMW) by solar TiO_2 photocatalysis and solar photo-Fenton, *Sol. Energy* 77 (2004) 567–572.
- [4] D. Vione, C. Minero, V. Maurino, M.E. Carloti, T. Picatotto, E. Pelizzetti, Degradation of phenol and benzoic acid in the presence of a TiO_2 -based heterogeneous photocatalyst, *Appl. Catal. B: Environ.* 58 (2005) 79–88.
- [5] K. Mehrotra, G.S. Yablonsky, A.K. Ray, Macro kinetic studies for photocatalytic degradation of benzoic acid in immobilized systems, *Chemosphere* 60 (2005) 1427–1436.

- [6] A. Di Paola, E. García-López, S. Ikeda, G. Marcí, B. Ohtani, L. Palmisano, Photocatalytic degradation of organic compounds in aqueous systems by transition metal doped polycrystalline TiO₂, *Catal. Today* 75 (2002) 87–93.
- [7] HACH, *Water Analysis Handbook*, 2nd ed., HACH Company, Loveland, 1992.
- [8] M.A. Miranda, F. Galindo, A.M. Amat, A. Arques, Pyrylium salt-photosensitised degradation of phenolic contaminants present in olive oil wastewaters with solar light. Part II. Benzoic acid derivatives, *Appl. Catal. B: Environ.* 30 (2001) 437–444.
- [9] M. Muneer, H.K. Singh, D. Bahnemann, Semiconductor mediated photocatalysed degradation of two selected priority organic pollutants, benzidine and 1,2-diphenylhydrazine, in aqueous suspension, *Chemosphere* 49 (2002) 193–203.
- [10] M. Muneer, D. Bahnemann, Semiconductor mediated photocatalysed degradation of two selected pesticide derivatives, terbacil and 2,4,5-tribromoimidazole, in aqueous suspension, *Appl. Catal. B: Environ.* 36 (2002) 95–111.
- [11] T. Ohno, K. Sarukawa, K. Tokieda, M. Matsumura, Morphology of a TiO₂ photocatalyst (Degussa P-25) consisting of anatase and rutile crystalline phases, *J. Catal.* 203 (2001) 82–86.
- [12] T. Velegraki, I. Poullos, M. Charalabaki, N. Kalogerakis, P. Samaras, D. Mantzavinos, Photocatalytic and sonolytic oxidation of acid orange 7 in aqueous solution, *Appl. Catal. B: Environ.* 62 (2006) 159–168.
- [13] J.M. Hermann, Heterogeneous photocatalysis: fundamentals and applications to the removal of various types of aqueous pollutants, *Catal. Today* 53 (1999) 115–129.
- [14] M.S.T. Goncalves, A.M.F. Oliveira-Campos, E.M.M.S. Pinto, P.M.S. Plasencia, M.J.M.S. Queiroz, Photochemical treatment of solutions of azo dyes containing TiO₂, *Chemosphere* 39 (1999) 781–786.
- [15] F. Kiriakidou, D.I. Kondarides, X.E. Verykios, The effect of operational parameters and TiO₂-doping on the photocatalytic degradation of azo-dyes, *Catal. Today* 54 (1999) 119–130.
- [16] B. Zielińska, J. Grzechulska, R.J. Kaleńczuk, A.W. Morawski, The pH influence on photocatalytic decomposition of organic dyes over A11 and P25 titanium dioxide, *Appl. Catal. B: Environ.* 45 (2003) 293–300.
- [17] A. Akyol, H.C. Yatmaz, M. Bayramoglu, Photocatalytic decolorization of Remazol Red RR in aqueous ZnO suspensions, *Appl. Catal. B: Environ.* 54 (2004) 19–24.
- [18] A.H.C. Chan, C.K. Chan, J.P. Barford, J.F. Porter, Solar photocatalytic thin film cascade reactor for treatment of benzoic acid containing wastewater, *Water Res.* 37 (2003) 1125–1135.
- [19] Y. Deng, K. Zhang, H. Chen, T. Wu, M. Krzyaniak, A. Wellons, D. Bolla, K. Douglas, Y. Zuo, Iron-catalyzed photochemical transformation of benzoic acid in atmospheric liquids: Product identification and reaction mechanisms, *Atmos. Environ.* 40 (2006) 3665–3676.
- [20] R.W. Matthews, Photo-oxidation of organic material in aqueous suspensions of titanium dioxide, *Water Res.* 20 (1986) 569–578.
- [21] R.W. Matthews, Photocatalytic oxidation of organic contaminant in water: an aid to environmental preservation, *Pure Appl. Chem.* 64 (1992) 1285–1290.
- [22] V.A. Sakkas, I.M. Arabatzis, I.K. Konstantinou, A.D. Dimou, T.A. Albanis, P. Falaras, Metolachlor photocatalytic degradation using TiO₂ photocatalysts, *Appl. Catal. B: Environ.* 49 (2004) 195–205.